Precession electron diffraction and its utility for structural fingerprinting in the transmission electron microscope

Peter Moeck[1], Sergei Rouvimov[1], and Stavros Nicolopoulos[2]

[1] Nano-Crystallography Group, Department of Physics, Portland State University, Portland, OR 97207-0751, U.S.A. & Oregon Nanoscience and Microtechnologies Institute, http://nanocrystallography.research.pdx.edu/index.py/nano_group

[2] NanoMEGAS SPRL, Boulevard Edmond Machterns No 79, Saint Jean Molenbeek, Brussels, B-1080, Belgium, http://nanomegas.com

Abstract

Precession electron diffraction (PED) in a transmission electron microscope (TEM) is discussed in order to illustrate its utility for structural fingerprinting of nanocrystals. While individual nanocrystals may be fingerprinted structurally from PED spot patterns, ensembles of nanocrystals may be fingerprinted from powder PED ring patterns.

Keywords: precession electron diffraction (PED), nanocrystals, structural fingerprinting

Introduction

For various reasons, structural fingerprinting of ensembles of nanocrystals is not feasible by means of standard laboratory-based powder X-ray diffractometry (XRD) [1]. Crystalline vanadium-oxide nanotubes [2], for example, show only one strong Bragg peak when a Cu-K_a X-ray tube is used for the recording of a powder X-ray diffractogram, Fig. 1. Because there is an industrial scale need for structural fingerprinting of nanocrystals, this paper discusses precession electron diffraction (PED) as an alternative to powder XRD.

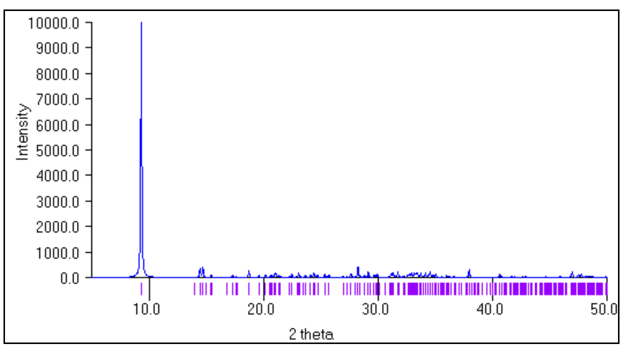

Fig. 1: Powder X-ray diffractogram of vanadium oxide nanotubes.

PED has existed for more than a decade [3] and found over recent year applications in electron crystallography [4]. This followed from the commercial availability of precession electron diffraction add-ons to existing TEMs* and because the structures of nanocrystals can be both solved and refined on the basis of PED data from individual nanocrystals. Any technique that facilitates the solving and refining of nanocrystals can also be used for structural fingerprinting [5,6].

The scattering of fast electrons in a TEM is particularly useful for structural assessments of nanocrystals. Since the interaction of the electrons with the periodic electrostatic potential in a crystal is several orders of magnitude stronger than the interaction of X-rays with the periodic electron density of the same crystal, this strong scattering necessitates the usage of the dynamical theory of electron diffraction in the routine practice of transmission electrum microscopy. For sufficiently thin nanocrystal, kinematic and quasi-kinematic approximations to the dynamical scattering theory do, however, frequently suffice [7-10].

The Blackman correction for primary extinction effects can be used for integrated reflection intensities in the two-beam dynamical case [9] and Bethe's dynamical potentials can be used in order to assess the influence of weak beams on strong beams [10]. Neither of these quasi-kinematic approximations requires the knowledge of the exact crystal thickness and orientation for its application. This feature makes them very useful for structural fingerprinting in the TEM.

Precession electron diffraction

The single-crystal PED method is formally analogous to the well known (single-crystal) X-ray (Buerger) precession technique. It utilizes, however, a precession movement of the primary electron beam around the microscope's optical axis rather than that of a zone axis of a single crystal around a fixed primary X-ray beam direction [3]. Due to the much larger radius of the Ewald sphere, the precession angles are in PED only a few degrees, i.e. an order of magnitude smaller than in X-ray precession. The primary electron beam can be either parallel or slightly convergent, and its precession creates a hollow illumination cone which has its vertex on the crystalline sample.

The primary electron beam and the diffracted beams are de-scanned (after they have left the nanocrystal) in such a manner that stationary diffraction patterns are obtained on the viewing screen of the TEM or on the recoding medium underneath this screen [3]. Figure 2 shows a sketch that illustrates the sequential creation of a single-crystal PED pattern.

The projection of the precession movement of the primary electron beam around the optical axis of the microscope onto the viewing screen of the TEM in direct space is equivalent to the rotation of the so called “Laue circle” in reciprocal space, Fig. 2. The circumference of the Laue circle represents the idealized locations of intersections of the Ewald sphere with zero-dimensional nodes of the reciprocal crystal lattice. Due to the small size of nanocrystals, these nodes are extended in three dimensions by the Fourier transform of the crystal shape function. Individual reflections of real nanocrystals that are located close to the circumference of the Laue circle are, therefore, excited more or less sequentially, Fig. 2, while the Laue circle as a whole rotates around the central *000* spot of the diffraction pattern.

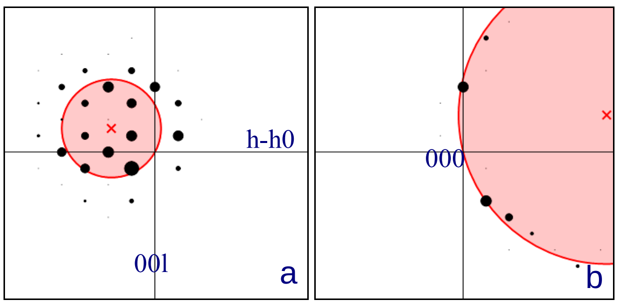

Fig. 2: Sketches to illustrate the sequential excitation of reflections in PED pattern, Si [110] zone axis, 200 kV, 10 nm crystal thickness. Note the effect of the increasing precession angle: 0.8° in (a) to 2.4° in (b).

The locations of the individual reflections on the diffraction pattern appear stationary as a result of the proper descaning of the diffracted beams, but their intensities vary while the Laue circle rotates (or equivalently the primary electron beam precesses). All reflections intersect the Ewald sphere twice per precession cycle, and (at least) partially integrated reflection intensities are recorded. Note that the locations of these reflections on the de-scanned (single-crystal) PED patterns are the same as those of their (non-integrated) counterparts in conventional (single-crystal), stationary-beam selected area electron diffraction (SAED) patterns, Figs. 3a and 4a. Because individual reflections are excited more or less sequentially while a PED pattern is building up, secondary dynamical scattering between simultaneously excited reflections is significantly reduced. For the same crystal thickness, the electron scattering conditions approach in the PED mode the two-beam dynamical diffraction theory much more closely than in the SAED mode.

Because PED reflection intensities are also (at least partially) integrated, the Blackman correction for primary extinction effects [9] is applicable for inorganic crystal with thicknesses of a few tens of nanometers [5,6]. Dynamical systematic row scattering is, however, not suppressed by the PED geometry since such rows tend to be excited at once [3,5,6].

The integration of the reflection intensities is more complete with larger precession angles. The thinner the crystal and the higher the precession angle, the more the reflection intensity distribution in an experimental PED pattern will approach Blackman’s predictions [9] for the two-beam dynamical case.

The radius of the Laue circle depends on the precession angle and can be calculated from the relation $R = |\vec{k}| \sin e$, where $|\vec{k}|$ is the magnitude of the electron wave vector in vacuum, and e the precession angle, i.e. the half angle of the hollow illumination cone of the precessing primary electron beam. An experimental PED pattern may extend in reciprocal space approximately to twice this radius. For 200 kV electrons and a precession angle of 2.8º, one obtains about 20 nm^{-1} for this extension, corresponding to a direct space resolution of 0.5 Å. This farther extension / increased resolution with respect to conventional SAED patterns may be understood as resulting from an “effective flattening of the Ewald sphere” and is illustrated by the experimental diffraction patterns of Figs. 3 and 4.

Figure 3 also shows that PED is experimentally less demanding than SAED since characteristic “zone axis diffraction patterns” can be obtained for crystals that are slightly mis-oriented. This is because the precession movement and proper descaning lead to an (at least partial) integration of the reflection intensities over the excitation error.

In addition, the integrated reflection intensities are modified by the prevailing Lorentz factors, which depend on the precession angle, crystal structure and thickness, as well as on the type of the crystalline sample [5-8]. As in X-ray diffraction, Lorentz factors account for the physical particulars (including the relative time intervals) of the intersections of the Ewald sphere with the shape transform of the nanocrystals at the accessible reciprocal lattice nodes.

For effects of the crystal thickness (and precession angle) on the integrated reflection intensities, compare Figs. 3b and 4b. While kinematically forbidden reflections are present in the experimental PED patterns of Figs. 3b and 4b, they can be differentiated from the other reflections by their characteristic intensity reduction with increasing precession angle [5,6].

Although the silicon crystal of Fig. 3 is approximately 60 nm thick, the reflection intensities in the PED patters may still be used for structural fingerprinting in either the quasi-kinematic or the asymptotic two-beam limit [7]. The reflection intensities of the approximately 6 nm thin silicon crystals of Fig. 4, on the other hand, can be treated kinematically as dynamical diffraction effects are negligible. This can be safely inferred from the very low intensity of the kinematically forbidden (002) and {222} reflections in Fig. 4a. On must, however, take the Lorentz factor into account for the PED pattern of the 6 nm thin silicon crystal. This is demonstrated by the clear visibility of the kinematically forbidden {222} reflections in Fig. 4b.

NSTI-Nanotech 2009, www.nsti.org, ISBN 978-1-4398-1782-7 Vol. 1, 2009

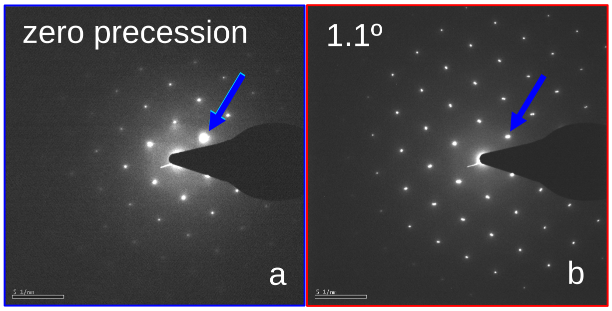

Fig. 3: Diffraction patterns from a silicon crystal, approximately 60 nm thickness, orientation close to [110], 200 kV. **(a)** SAED pattern (zero precession), **(b)**, PED pattern from the same area. Note that while the intensity of the $(1\bar{1}\bar{1})$ reflection, marked by arrows, is much higher than that of its Friedel pair $(\bar{1}11)$ and that of the other two symmetry equivalent $\pm(1\bar{1}1)$ reflections in the SAED pattern (a), the intensities of all four {111} reflections are very similar in the PED pattern.

Because the reflection intensities are (at least partially) integrated, the projected Laue class symmetry in the PED patterns can be made another component of structural fingerprinting. Due to the large curvature of the Ewald sphere, the possible Laue classes of the reflections in the zero order Laue zone all contain a two-fold rotation axis. One can, therefore, only distinguish between those six 2D point groups that contain a two-fold axis, i.e. 2, 2mm, 4, 4mm, 6 and 6mm. The other four 2D point groups that do not contain such an axis, i.e. 1, m, 3, and 3m, are possible for reflections in higher order Laue zones, since {h k l+1} and {-h -k -l+1} reflections are not Friedel pairs. Note also that the Laue class symmetry of PED patterns that were recorded with large precession angles is rather insensitive to the exact crystal orientation and dynamical diffraction effects. It is, therefore, a valuable characteristic that can be employed advantageously for structural fingerprinting from PED patterns.

Since kinematically forbidden reflections can be identified from a series of PED patterns with increasing precession angle [5,6], space group information may be inferred from them [11]. Reflections from higher order Laue zones in large precession angle PED patterns are particularly useful for this purpose and the space group information determination can be utilized as a third additional component of structural fingerprinting of individual nanocrystals in the TEM [5,6]. This is all in addition to traditional structural fingerprinting of individual single-crystals from SAED patterns where only the projected reciprocal lattice geometry, i.e. the two shortest reciprocal spacings and the interplanar angle have been utilized [1].

Note that structural fingerprinting from PED patterns of individual nanocrystal has recently been automated* and highly reliable crystal orientation and phase maps can be recorded in a TEM from a μm^2-sized sample-area within minutes [12]. Note that the spatial resolution of these maps is superior to the maps that can be recorded by means of the electron backscattering (Kikuchi line) technique in a scanning electron microscope. In addition, electron spot diffraction in a TEM is much less sensitive to the plastic deformation state and possible surface structures of nanocrystals than Kikuchi line backscattering.

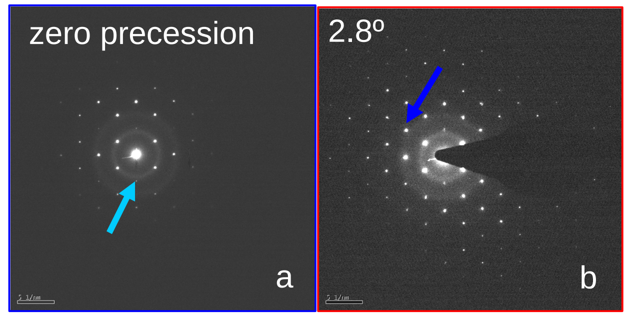

Fig. 4: Diffraction patterns from an approximately 6 nm thin section of a wedge shaped silicon crystal in [110] orientation, 200 kV. **(a)** SAED pattern (zero precession). **(b)** PED pattern from the same area. While the (barely visible) kinematically forbidden (002) reflection is marked by an arrow in (a), the arrow in (b) marks the kinematically forbidden $(\bar{2}2\bar{2})$.

Just as SAED patterns, e.g. Fig. 5a, can be recorded from a whole ensemble of nanocrystals at once, Fig. 5b, PED patterns may be recorded from crystalline samples of this type as they do possess advantages for structural fingerprinting in the TEM.

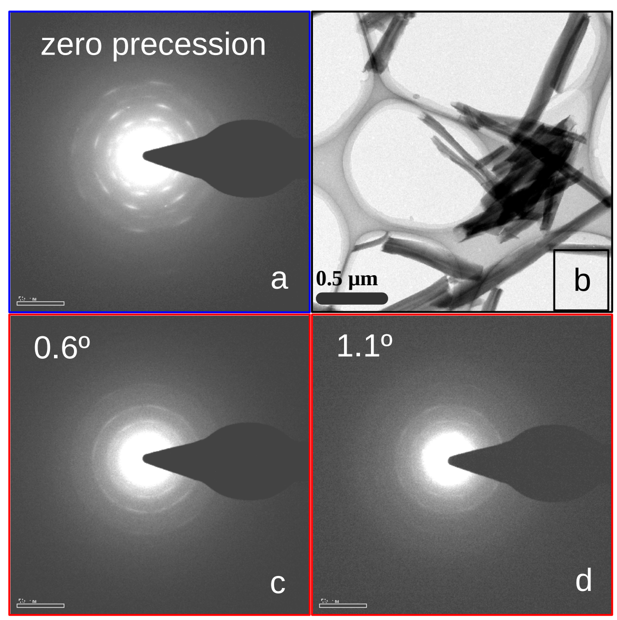

Fig. 5: Structural fingerprinting of an ensemble of crystalline vanadium-oxide nanotubes [2], 200 kV. **(a)** powder SAED pattern, **(b)** bright field image, **(c)** and **(d)** powder PED patterns with increasing precession angle.

Figures 5c and 5d show, for example, "powder PED patterns" from vanadium-oxide nanotubes [2], i.e.

crystalline nanotubes that cannot be fingerprinted structurally from powder XRD, Fig. 1. As can be appreciated from the qualitative comparison of Fig. 5a with Figs. 5b and 5c, the powder PED mode leads to an effective suppression of texture effects.

Figures 6 and 7 shows powder SAED and PED patterns of Zeolite Socony Mobil #5 (ZSM-5) and Ni-doped cassiterite (SnO_2) nanocrystals. The Debye-Scherrer rings are more clearly revealed in the precession pattern. This is due to a better statistical crystallite orientation assessment as more nanocrystals contribute integrated intensities to the latter type of pattern. Both of increased visibility of Debye-Scherrer rings and the texture suppression effects support structural fingerprinting in the TEM [1].

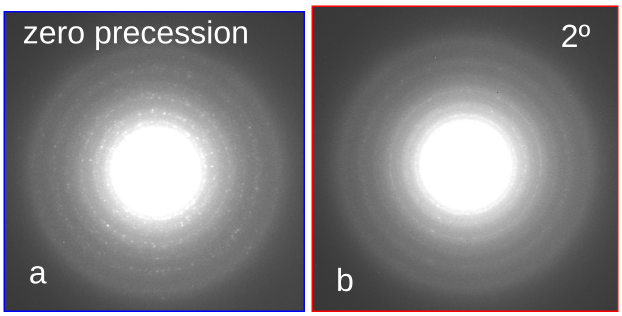

Fig. 6: Powder SAED **(a)** and PED **(b)** patterns of Zeolite Socony Mobil #5 (ZSM-5), 100 kV.

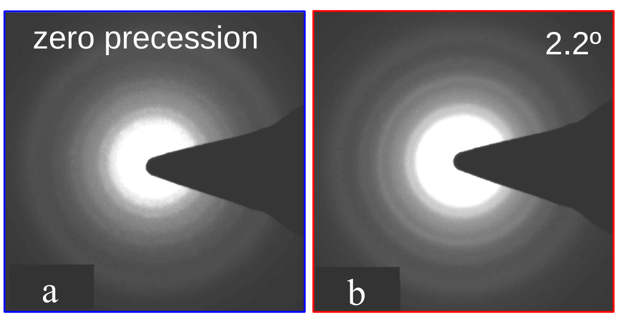

Fig. 7: Powder SAED **(a)** and PED **(b)** patterns of Ni-doped cassiterite (SnO_2) nanocrystals, 200 kV.

Summary and Conclusions

Precession electron diffraction results in quasi-kinematic integrated reflection intensities for inorganic crystals that are up to several tens of nanometers thick. Lorentz factors need to be employed for the correct interpretation of these reflection intensities. Structural fingerprinting in the TEM can be significantly enhanced by the utilization of commercially available* add-on instrumentation to existing mid-voltage TEMs.

Acknowledgments

This research was supported by awards from the Oregon Nanoscience and Microtechnologies Institute. Additional support from Portland State University's Venture Development Fund is acknowledged. We thank Prof. Valeri Petkov of Central Michigan University for the vanadium-oxide nanotube sample and Prof. Daniel R. Gamelin of the University of Washington for the cassiterite sample.

References

[1] Moeck, P.; Fraundorf, P.: Structural fingerprinting in the transmission electron microscope: Overview and opportunities to implement enhanced strategies for nanocrystal identification, *Zeits. Kristallogr.* **222** (2007) 634-645, expanded version at: arXiv:0706.2021; **open access:** at the journal's web pages: http://www.atypon-link.com/OLD/toc/zkri/222/11?cookieSet=1

[2] Petkov, V.; Zavalij, P. Y.; Lutta, S.; Whittingham, M. S.; Parvanov, V.; Shastri, S.: Structure beyond Bragg: Study of V_2O_5 nanotubes, *Phys. Rev. B* **69** (2004) 85410.

[3] Vincent, R.; Midgley, P.: Double conical beam-rocking system for measurement of integrated electron diffraction intensities, *Ultramicroscopy* **53** (1994) 271-282

[4] Zou, X. D.; Hovmöller, S.: Electron crystallography: imaging and single-crystal diffraction from powders, *Acta Cryst. A* **64** (2008) 149-160; **open-access:** http://journals.iucr.org/a/issues/2008/01/00/isscont s.html

[5] Moeck, P.; Rouvimov, S.: Structural fingerprinting of nanocrystals in the transmission electron microscope: utilizing information on projected reciprocal lattice geometry, plane group symmetry, and structure factors, ***in:*** *Nano Particle Drug Delivery Systems: II Formulation and Characterization*, Y. Pathak and D. Thassu (editors), Informa Health Care, New York, 2009, *in press*

[6] Moeck, P.; Rouvimov, S.: Precession electron diffraction for structural fingerprinting of nanocrystals in the transmission electron microscope, *Zeits. Kristallogr.* (2009) *in press*

[7] Vainshtein, B. K.: *Structure Analysis by Electron Diffraction*, Pergamon Press Ltd., Oxford, 1964.

[8] Vainshtein, B. K.; Zvyagin, B. B.: Electron-diffraction structure analysis, ***in:*** *International Tables for Crystallography*, Vol. **B**, Reciprocal space, Ed. U. Shmueli, 2nd edition, Kluver Academic Publ., Dordrecht, 2001, pp. 306-320.

[9] Blackman, M.: On the intensities of electron diffraction rings, *Proc. Royal Society (London)* A **173** (1939) 68-82.

[10] Klechkovskaya, V. V.; Imamov, R. M.: Electron Diffraction Structure Analysis - from Vainshtein to Our Days, *Crystallography Reports* **46** (2001) 534-549.

[11] Morniroli, J. P.; Redjaïmia, A.: Electron precession microdiffraction as a useful tool for the identification of the space group, *J. Microsc.* **227** (2007) 157-171.

[12] Rouvimov, S.; Rauch, E. F.; Moeck, P; Nicolopoulos, S.: Automated Crystal Orientation and Phase Mapping of Iron Oxide Nano-Crystals in a Transmission Electron Microscope, *this conference proceedings*

* NanoMEGAS SPRL offers such devices and Portland State University's "Laboratory for Structural Fingerprinting and Electron Crystallography" (run by Prof. Peter Moeck) serves as the first demonstration site of this company in the Americas. A precession electron device "Spinning Star" is installed there on an analytical FEI Tecnai G^2 F20 ST field-emission transmission electron microscope and can be demonstrated on request.